Chemistry, radiation, aerosols and clouds in the atmosphere of Córdoba City

Maria Laura López[1], *Mariana Achad*[1], *Luis E. Olcese*[1], *Gustavo G. Palancar*[1*] *and* ***Beatriz M. Toselli*** [1*]

1.Departamento de Físico Química / INFIQC / C LCM/ Facultad de Ciencias Químicas, Universidad Nacional de Córdoba. Ciudad Universitaria, 5000 Córdoba. ARGENTINA

Environmental context

This chapter presents the main results of the advances made in the central region of Argentina respect to the different environmental aspects of radiation, aerosols and clouds. UV-B radiation reaching the ground is the driving force of the photochemical reactions responsible of air pollution and global warming of the planet. In addition, a strong association between aerosol pollution and mortality rates was reported leading to World efforts to reduce their levels. In this context, the local situation is discussed.

Abstract

Ultraviolet-B radiation (UV-B, 280-315 nm) is monitored in Córdoba, Argentina (31º 24' S, 64º 11' W, 400 m above sea level) using a Yankee Environmental Systems (YES) pyranometer, model UVB-1. Measurements of solar broad band UV-B irradiances are conducted since November 1998. These are, to our knowledge, the first measurements obtained in Córdoba with a high quality pyranometer. For clear sky days, the measurements are in good agreement with results of a radiative transfer model. However, this study shows substantial reductions of UV-B radiation on cloudy days and days with high levels of particle matter. These two effects are comprehensively addressed in this chapter. The effects of cumulus, cirrus, and stratocumulus clouds on surface radiation are specifically analyzed. In addition, the effect of aerosols on air quality is addressed measuring the monthly concentration of PM10 (2009-2010) and PM2.5 (2009-2011) and the average chemical composition (2009-2010) by means of the Synchrotron radiation X-ray fluorescence technique (SR-XRF). Electronic microcopies (TEM, SEM) are used to analyze individual particles and provide complementary information on shape, size and chemical composition.

1. Introduction

UV sunlight drives the chemistry of the atmosphere. As such, it is important to understand the magnitude and variability of the solar irradiance reaching the ground and the mechanisms that controls its transmission through the atmosphere. This knowledge is essential not only for chemistry (assessment of the photolysis rate constants) but also for many other fields such as health, agriculture, meteorology, etc. In order to assess the amount of UV radiation reaching a specific place at the Earth's surface a number of factors should be considered. Clouds are one of the most important factors influencing radiation. Because they are formed by water droplets or ice crystals, radiation is scattered when passing through them, resulting in extinction or in a

[*] To whom correspondence should be addressed.
palancar@fcq.unc.edu.ar, tosellib@fcq.unc.edu.ar,
Departamento de Físico Química / INFIQC
Facultad de Ciencias Químicas
Universidad Nacional de Córdoba
Pabellón Argentina. Ciudad Universitaria.
5000. Córdoba. Fax: +54 351 4334188
ARGENTINA.

diminished atmospheric transmissivity. McKenzie et al. [1] reported attenuations of 25-30% in the global UV reaching the ground; Lubin et al. [2] found attenuations of 10-25% in the rain forest, and Estupiñán et al. [3] noted that attenuation may be undetectable for very thin clouds or small cloud amount but may be as high as 99% under extremely thick clouds.

Besides clouds, aerosols and pollutants absorb and scatter shortwave solar radiation and these interactions have resultant impacts on atmospheric radiative transfer balance. It is even believed that they can partially offset the increase of UV radiation from stratospheric ozone depletion (Frederick et al., [4]; Meleti and Cappellani[5]). Atmospheric aerosol particles in the boundary layer can also significantly change air quality either directly or by affecting the rate of tropospheric ozone formation. Scattering by aerosols increases the actinic flux and the rates of photochemical reactions in the upper parts of the planetary boundary layer, while aerosol absorption reduces the amount of UV radiation available for chemical reactions within and below the aerosol layer. Therefore, without accurate knowledge of aerosol UV absorption, the magnitude and even the sign of the aerosol effect on tropospheric photochemistry will remain highly uncertain. Scattering and absorption of solar radiation by aerosol particles and gases results in a remarkable attenuation of direct solar beam component and in a moderate increase in diffuse component. The net result is a decrease in global (direct and diffuse) irradiance that reaches the ground. The effect of tropospheric aerosols on UV radiation varies widely in time and space due to their short residence time (2–7 days), variability in size, shape, chemical composition, and dependence on relative humidity. This is because scattering and absorption properties of aerosols have strong dependence with these factors. It was found that more than 80% of the aerosol effect on UV radiation due to increasing turbidity is determined by aerosol optical depth (AOD) and single scattering albedo (ω_o) (Reuder and Schwander[6]). The latter is the ratio of the aerosol scattering coefficient to the total aerosol extinction coefficient (scattering plus absorption). Many studies have obtained values for ω_o in the visible wavelengths for specific locations and times (Anderson et al. [7]; Devaux et al. [8]; Dubovik et al. [9]); however, less research has been done to determine values of ω_o in the UV wavelengths (Krotkov et al. [10]; Kylling et al. [11]). Madronich[12] and Lacis and Mishchenko[13] stated that in the UV spectrum ω_o varies between 0.5 and 1.0, depending on particle composition. Dust and soot aerosols tend to have lower values (0.5 to 0.7), while sulfate aerosols have values closer to 1.0. Indirect methods for the determination of the aerosol properties from solar irradiance have been proposed and tested, using either global or direct irradiance measurements (Kazadzis et al.[14]; Bais et al. [15]), or the direct-to-diffuse irradiance ratio at selected wavelengths (Goering et al. [16]; Slusser et. al. [17]).

Apart from its effect on radiation, aerosols affect air quality and therefore it is important to characterize them from a chemical point of view. The toxicity of the particles is associated not only to higher mass of particulate matter, but also to variations in particle size, shape, and chemical composition. Furthermore, many trace chemical species in particles occur in the very fine size fractions, which can reach alveolar regions in the lungs. High levels of PM10 and PM2.5 (particulate matter with aerodynamic diameter less than 10 and 2.5 μm, respectively) have been shown to decrease pulmonary function and exacerbate respiratory problems in respiratory-compromised people, i.e., asthmatics. A strong association between the fine air particulate pollution and mortality rates in six U.S. cities has been also reported (Dockery and Pope[18]).

Two different approaches can be used to analyze the chemical composition of the aerosols: bulk and single particle analysis. For bulk analysis, plasma based methods such as inductively coupled plasma optical emission spectrometry (ICP-OES), and inductively coupled plasma-mass spectrometry (ICP-MS) are the most used techniques for routine aerosol multi-elemental characterization (Smichowski et al. [19]; Suzuki[20]). Synchrotron radiation X-ray fluorescence (SR-XRF) is another powerful tool used to characterize aerosols as it allows to analyzing samples with complex mixtures and low concentrations. For single particle analysis, microscopic electronic techniques such as TEM and SEM coupled with EDX analysis are widely used.

The aim of this chapter is to present the main results of the advances made in the central region of Argentina respect to the different environmental aspects of radiation, aerosols and clouds mentioned above.

2. Methodology

2.1 Experimental section

To quantify the effect of aerosols and clouds on surface UV-B radiation it has been used two pyranometers YES (Yankee Environmental System, Inc.) model UVB-1, a pyranometer YES model TSP-700, an Ocean Optics USB4000 spectrometer, and a CIMEL Sun photometer. The first two instruments are mounted on a wide-open area in the University Campus in Córdoba City (Argentina, 31º 24' S, 64º 11' W, 470 m a.s.l.), which can be considered as a semi urban location. The former measures UV-B global irradiance (280-315 nm), while the latter measures total global irradiance (300-3000 nm). The measurement site and the UVB-1 spectral response function have been discussed in greater detail elsewhere (Olcese and Toselli[21]; Palancar and Toselli[22], respectively). Both, UVB-1 and TSP- 700 sensors were factory calibrated. Cloudless conditions were periodically assured by direct observers. The optical properties of aerosols are measured world-wide by AERONET (AErosol RObotic NETwork), which is a federated international network, coordinated by the NASA Goddard Space Flight Center. Near Córdoba City, a CIMEL Sun photometer, which is part of this network, was deployed at Córdoba CETT (Centro Espacial Teófilo Tabanera; 31º 30' S, 64º 24' W)) between 1999 and 2010. This solar photometer allows to directly considering the characteristic of local aerosols in model calculations through the aerosol optical depth (AOD), single scattering albedo (ω_o), and asymmetry factor (g) parameters. AOD is the only measured parameter, while the others are obtained through mathematical inversion methods. These optical properties are reported in seven spectral bands (340, 380, 440, 500, 670, 870 and 1020 nm) and they can be downloaded from the website: http://aeronet.gsfc.nasa.gov. A detailed description of the instruments and data acquisition procedure was given by Holben et al. [23] An accuracy assessment of the AERONET retrievals can be found in the work of Dubovik et al. [24] The National Observatory of Córdoba provided additional meteorological data.
The DPS system with the SKC impactor was employed for sampling PM2.5 and PM10. An inertial impactor removed particles larger than a specific cut-point by capturing them on a disposable 37-mm pre-oiled porous plastic disk that reduces particle bounce. A flow rate of 10 L/min was employed to ensure the maximum efficiency of the instrument. For bulk chemical analysis (SR-XRF), particles were collected on a 47-mm PTFE filter during 24 hours during the years 2009-2012, while for single particle analysis (TEM and SEM-EDX), SPI formvar coated 200-mesh copper grids were used. SR-XRF was used to determine the chemical composition of aerosol particles at the Brazilian National Synchrotron Light Laboratory (LNLS). The measurements were carried out using the D09B-XRF beamline. Aerosol samples were excited with both white and monochromatic beam at different energies. TEM analysis was done by using a JEOL JEM 1200 EX II transmission electron microscope operating at an accelerating voltage of 80 kV. The magnifications ranged from 6000 up to 80000X. The samples were collected during the years 2007-2009, covering a wide range of meteorological conditions. SEM images were recorded with a LEO 1450VP Scanning Electron Microscope employing a combination of secondary and backscattered electrons. The magnifications ranged from 1000 up to 15000X. Prior the analysis, the grids were mounted on an Al-stub using a conductive double-sided adhesive tape.

2.2 Model calculations

2.2.1 Air mass transport model

The dynamical aspects of the meteorology in the central region of Argentina were studied by means of the HYSPLIT (HYbrid Single-Particle Lagrangian Integrated Trajectory) model). This model was designed by the Bureau of Meteorology of Australia and the ARL-NOAA of USA

(Draxler and Hess[25]) and is commonly used to modeling a wide range of conditions related to the regional or long-range transport, dispersion, and deposition of air pollutants. It uses a hybrid approach, in which the calculation employs puff distribution in the horizontal direction and particle dispersion in the vertical (Draxler[26]). HYSPLIT calculates advection and dispersion using either puff or particle approaches under a Lagrangian framework. The transport and dispersion of a parcel is calculated by assuming the release of a single puff that will expand, and then it will split into several puffs when its size exceeds the meteorological grid cell spacing (1º x 1º in our calculations). The trajectory calculation is achieved by the time integration of the position of an air parcel as it is transported by the wind field. HYSPLIT can be also used to calculate the source region of an air parcel by moving backward in time, thus indicating its arrival at a receptor at a particular time. Many studies employs HYSPLIT backtrajectory analysis in a variety of aerosol and particles related studies (Vana and Tamm[27]; Gassmann and Pérez[28]; McGowan and Clark[29]). The meteorological dataset used in this work was the Global Data Assimilation System (GDAS) (NOAA, 2003) from National Centers for Environmental Prediction (NCEP), that uses a global 1º x 1º grid (360 by 181) and 12 pressure levels, up to 50 hPa, with a temporal resolution of 3 hours.

2.2.2 Radiative transfer model

The Tropospheric Ultraviolet and Visible (TUV) radiation model version 4.1 was used for all UV-B calculations (Madronich[30]; Madronich and Flocke[31]). A sensitivity analysis was carried out on this model in order to establish the best values for the most important parameters in the calculations for Córdoba City (Palancar[32]). The final setup used in the model was as follows: the wavelength grid was built with 1 nm intervals between 280 and 315 nm; the surface albedo was assumed to be Lambertian, wavelength-independent, and with a constant value of 0.05 throughout the year; the extraterrestrial irradiance values were taken from Van Hoosier et al. [33] and Neckel and Labs[34], and an 8-stream method was selected. Due to the low levels of tropospheric UV-B absorbing pollutants like O_3, SO_2, and NO_2 in Córdoba City (Olcese and Toselli[35]), they have not been considered in the calculations. Total ozone column values were obtained daily by the Total Ozone Mapping Spectrometer (TOMS) instrument onboard Earth Probe spacecraft and were provided by the Ozone Processing Team of the Goddard Space Flight Center of the National Aeronautic and Space Administration (NASA, United States). The default aerosol profile included in the model was taken from Elterman[36]. These data were obtained for 340 nm, so it is assumed that optical depth scales inversely with first power of wavelength.

3 Results and discussion

In the following subsections the most important results respect to air mass transport, effects of clouds and aerosols on radiation, and gravimetrical and chemical analysis of the aerosols, are presented.

3.1 Air mass transport

As it was mentioned, Córdoba faces air pollution problems, mainly during wintertime. Strong radiative inversions occur during winter due to long nights, dry air and cloudless skies. Because of that, pollutants and aerosols can be trapped in a layer lower than 200 meters, leading to high concentrations of several species and the consequent adverse effects on health. This fact is aggravated because during winter time, serious fires, caused accidentally or intentionally, break out on the hills that border the city to the west. The plume caused by the fires usually reaches the city and causes deterioration of the visibility and the air quality. These and other aspects of the dynamics of the region were investigated using the HYSPLIT model. The model was used to analyze and correlate the origin of the air masses with the aerosols collected in Córdoba. Back trajectories were calculated to obtain the place where the air mass was located 24 hours before arriving to the measurement site. Then, these locations were grouped depending on its position in a grid, which is spaced every 30 kilometers in both latitude and longitude (*Figure 1*).

From the *figure 1* is observed that, 24 hours before arriving to the site, the air masses are mostly located towards the northeast. Although *figure 1* shows the behavior during the whole year (2009), a similar pattern has been observed for each month.

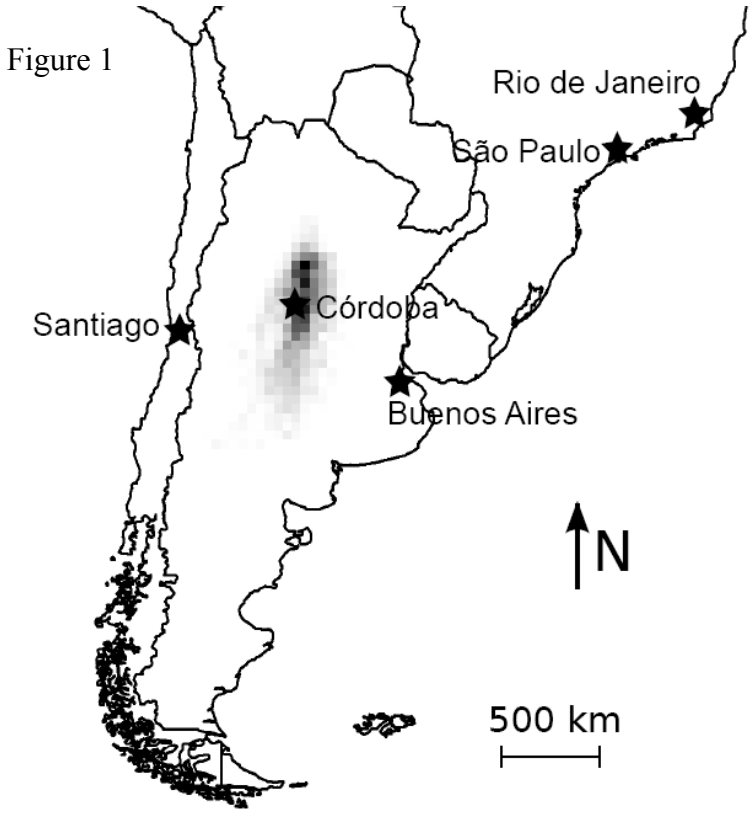

Figure 1: 24 hours back-trajectories averaged during the whole 2009 year calculated by the HYSPLIT transport model.

3.2 Irradiance measurements in presence of clouds

The effects of different types of clouds (stratocumulus, cumulus, and cirrus) on the broadband UV-B irradiance have been analyzed and differentiated by using model calculations and surface measurements taken in Córdoba City, Argentina.

Different theoretical and empirical parameterizations have been proposed to quantify the effect of clouds on UV radiation. One of them is the Cloud Modification Factor (CMF) defined as the ratio between the measured radiation in a cloudy sky and the calculated radiation for a cloudless sky (e.g. López et al. [37]); other one is the ratio between diffuse and global radiation (DGR) (López et al. [38]). Here the results obtained through the use of DGR are presented for a total of 16 days with stratocumulus, 12 with cumulus, 16 with cirrus and 21 clear sky days as a reference. These types of clouds were selected because of their different microphysical properties (liquid/ice water content, particle effective sizes, and distribution of water/ice particles) which determine their optical characteristics affecting the absorption and scattering of solar radiation.

DGR was specifically defined as:

$$DGR = \frac{UVB_{diffuse}}{UVB_{global}}$$

where $UVB_{diffuse}$ and UVB_{global} denote diffuse and global UV-B irradiances, respectively.

To perform the calculations with the TUV model under cloudy conditions a high resolution altitude grid was used. The Earth atmosphere was divided in 800 equally spaced layers (10 m

thick) up to 8 km a.s.l. The cloud optical parameters used in the model were as follows: g = 0.85; ω_o = 0.9999; and optical depth (τ) = variable between 1 and 30. A 1 km thick cloud was placed at 1.0 km above the surface because it is a frequent height for stratocumulus clouds (e.g. Zuidema et al., 2009[39]).

The analysis (diffuse and global irradiance, average and standard deviation of the DGRs, behavior of the DGR as a function of the SZA) led to a clear differentiation of the effects of each type of cloud. The found averages and standard deviations for the DGRs were 1.02 ± 0.06 for stratocumulus, 0.74 ± 0.18 for cumulus, 0.63 ± 0.12 for cirrus, and 0.60 ± 0.13 for the clear sky days, respectively. The results show the large effect of the stratocumulus and the relatively little effect of cirrus on the distribution of the UV-B irradiance at surface. Besides, stratocumulus clouds showed a low variability in the DGR values, which were concentrated close to 1 at all SZAs. DGR values for cumulus clouds presented a large variability at all SZAs mostly associated with the different optical depths. Finally, the closeness between the DGR values for cirrus clouds and the DGR values for clear days showed that these clouds generally do not strongly affect the UV-B irradiance at surface at any SZAs. In general, the radiation path through the cloud (which in turn depends on the SZA, the cloud optical depth, and the morphology of the cloud) determines the distribution of the irradiance components. At large SZAs (low Sun) the DGRs are mostly determined by the path length through the atmosphere (Rayleigh scattering) and not by the clouds. This study was carried out to contribute to the understanding of the radiation-cloud interactions in the UV-B range, a subject of essential importance in the evaluation of photolysis processes and in the development of realistic radiative transfer schemes and chemistry-transport models.

3.3 Irradiance measurements in the presence of aerosols

Palancar and Toselli[40] showed that the agreement between UV-B irradiance measurements and TUV model calculations under clear-sky conditions is better than ±5% for SZA less than 50º and better than ±10% for SZA less than 70º. That means that larger reductions can be attributed to the effect of the aerosol loading on the UV-B radiation. This effect was incorporated by means of AOD (340 nm), ω_0 (440 nm) and g (440 nm) values provided by AERONET, to simulate the experimental UV-B irradiance with the TUV model. Although ω_0 (440 nm) and g (440 nm) differs from that at 340 nm it should be noted that the lowest wavelength at which these parameters are available from AERONET is 440 nm. Thus, both factors are assumed constant from 440 nm down to 340 nm in model calculations. Comparison between experimental and modeled irradiance for specific days showed a very good agreement once the optical parameters provided by AERONET have been incorporated in the TUV model (Andrada et al. [41]). *Figure 2* shows the ratio between measurements and model calculations at solar noon only for cloudless days from the end of 1998 up to the end of 2012.

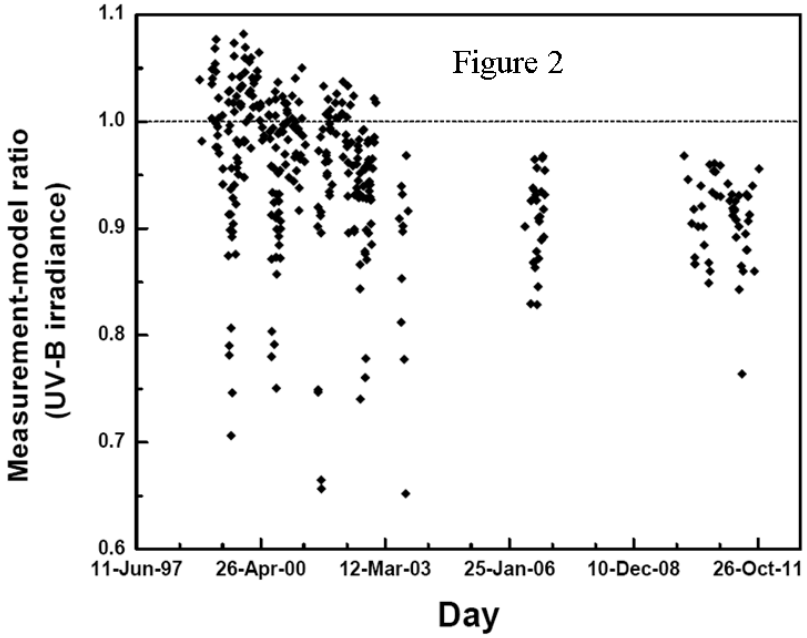

Figure 2: Annual and interannual variation of UV-B irradiance plotted as the ratio between measurements and calculations at solar noon. In order to see the aerosol loading effect only cloudless days were included.

The observed gap corresponds to a period where no measurements are available. As it can be seen, a systematic and important reduction in UV radiation is measured from August to November each year. The attenuation of the UV-B radiation is often observed in late winter and spring due to the particular meteorology of Córdoba City (Olcese and Toselli[42]; Palancar and Toselli[43]). It is important to keep in mind that these months are characterized by strong winds blowing during most of the day and with variable direction. Levels of relative humidity are low and considerable amount of geological particulate is present during most of the month. Hence, the determining factors for this behavior are the strength of the winds and the lack of rain. As a consequence of this combination, particulate matter is not removed from the atmosphere and it results in the systematic reduction in UV-B levels observed during every winter-spring period. The horizontal line in figure 2 indicates the ratio equal to one, which means a perfect measurement-model agreement. After many days without rain, reductions can reach up to 36% and after a rain the relation returns to values near to 1. All the values higher to 1 are within the mentioned measurement-model agreement. Here, it should be mentioned that SZA at noon in Córdoba varies between 7.9º and 54.9º. Thus, all SZA values fall well within the interval where the agreement is better than ±10%. In general, the differences might have its origin mainly in the ozone column value as this value is provided by TOMS team only once a day but it is used for calculations along the whole day. Other factors which may contribute to these differences are experimental uncertainties, model approximations, subvisible clouds, or a small aerosol loading.

3.4 Gravimetric analysis of the aerosols

The increasing evidence indicating that fine particulate matter in the atmosphere is responsible for adverse effects on humans led to the imposition of regulative restrictions on PM2.5 and PM10. Thus, The United States adopted a National Ambient Air Quality Standard (NAAQS), which sets two standards for 24-hour average: a limit of 150 μg m^{-3} for PM10 and 35 μg m^{-3} for PM2.5, respectively. On other hand, the European Union (EU) legislation for air quality established a 24-hour limit value of 40 μg m^{-3} for PM10 and 25 μg m^{-3} for PM2.5.

As it was shown by Olcese and Toselli[42] particulate matter measured as PM10 was the only air quality parameter that exceeded the Argentinean National Limits during the period 1994-2001 measured by the Undersecretary of Environment of Córdoba City. Therefore we decided

to evaluate the total mass of PM10 and PM2.5 and compare them with the international standards.

In order to evaluate the total mass concentration of PM10 and PM2.5, aerosol samples were collected during 2009 and 2010 at one urban and one semi-urban site. PM2.5 fraction weighted in the average 68.4 ±18 μg m^{-3} and 57±18 μg m^{-3} respectively, whereas the samples of the same sites in the PM10 fraction weighted 101±29 μg m^{-3} and 98±14 μg m^{-3}. The monthly PM values are presented in *table 1*, along with the monthly precipitation values.

Month	*PM10 Semiurban*	*PM2.5 Semiurban*	*PM10 Urban*	*PM2.5 Urban*	*Precipitation (mm)*
Jun 09	-	-	-	-	5
Jul 09	-	61	92	81	0
Aug 09	101	54	65	43	0
Sep 09	105	49	109	82	30
Oct 09	120	71	108	113	11
Nov 09	102	37	135	63	135
Dec 09	-	91	-	-	117
Jan 10	-	-	127	74	66
Feb 10	112	93	100	70	175
Mar 10	81	53	87	78	132
Apr 10	85	56	89	55	49

Table 1. Monthly averages of PM10 and PM2.5 concentrations (μg m^{-3}) and precipitations (mm)

During the period of measurements both fractions of particulate were very high with no clear trend at one particular season. These results seem to be surprising at first sight, but we have attributed it to the extremely dry 2009 year, with a precipitation 200 millimeters lower than the annual average. The ratio PM2.5/PM10 is 0.64 and 0.59 for each site respectively, indicating that fine particles PM2.5 dominates in PM10. The highest ratio was found in the most polluted urban site, although the PM2.5/PM10 values presented little variability for the two sites. This result might suggest that the contributions of coarse particles (PM10-PM2.5) and fine particles (PM2.5) are similar. Similar values have been reported in a large number of urban and semi-rural US areas where annual mean PM2.5/PM10 ratios varied between 0.3 and 0.7 (USEPA, 2004[44]). Note that the concentration of the PM2.5 fraction exceeds by far the value of the NAAQS and EU standards.

Because it has been shown that PM2.5 is the fraction most dangerous to human health, from 2010-2012 we decided to focus only on the measurement of this fraction at one site. This site was selected because its particular characteristics, as it receives the influence of air masses coming from downtown where most of the mobile sources are present, and has important areas of bare soil. *Figure 3.a* shows the monthly and inter-annual variation of PM2.5 fraction at the semi-urban site during the whole period. Figure 3.b shows the monthly precipitation. Note that there is correlation between the lack of precipitation and the loading of particulate matter in the atmosphere of Córdoba City. [45]

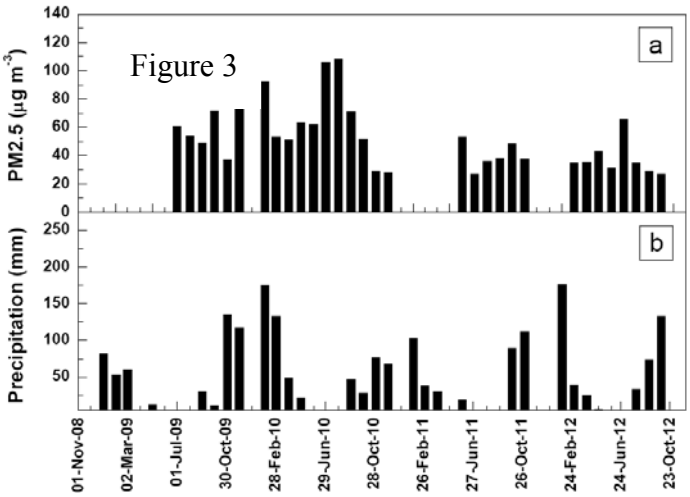

Figure 3: a) PM2.5 monthly average concentration for the years 2009-2012. **b)** Monthly average precipitation for the same period.

3.5 Chemical analysis of the aerosols
3.5.1 Bulk elemental Concentration

It has been shown that the chemical elements derived from anthropogenic sources are usually present in the fine fraction while those derived from natural sources are usually present in the coarse fraction. Suspended road dust and soil dust are other potential source of natural aerosols. *Figure 4* summarizes the average concentration values of the detected elements in the two fractions and at an urban and a semi-urban sites obtained by SR-XRF. From the figure, it can be observed that at the two sites the absolute concentration of the various elements is highly differentiated, ranging from a few ng m^{-3} for Co and Ni up to some μg m^{-3} for Si, Ca, Fe and K. The elements have different behaviors not only in their absolute concentrations but also in the relative sharing in the two fractions that constitute PM10. The typical crustal elements Al, Si, K, Ca, Ti, V, Mn, Fe and Ba were detected mostly in the coarse fraction (PM10-PM2.5). On the other side, S, Cr, Co, Ni y Zn elements presented similar concentration in both fractions. For the urban site Pb and Al were found in both, PM10 and PM2.5 fractions. [45]

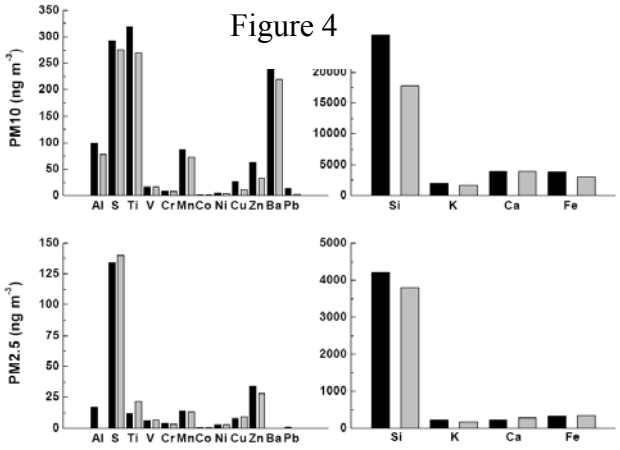

Figure 4: Average concentrations of minor and major elements determined by SR-XRF from PM10 (upper panel) and PM2.5 (lower panel) at the two monitoring sites from July 2009 to April 2010. Black bars correspond to the urban and grey bars to the semi-urban sites, respectively.

3.5.2 Single particle elemental characterization

SEM-EDX analysis was used to characterize the chemical composition of particles collected at the two sites. The EDX analysis reveals that Córdoba atmosphere contains a wide range of particle sizes and chemical elements. Here it should be mentioned that one of the limitations of the SEM-EDX technique is that volatile material will evaporate in high vacuum inside of the SEM chamber. This may cause some particles to shrink, deform, or even disappear completely. Particles, potentially affected by this problem have not been treated in any specific way as part of the analysis. High-energy electron beam can cause further damage or deformation on aerosol particles during EDX analysis. The particles chosen for elemental analysis were selected manually, based on the secondary electron image. The net intensities of the EDX spectra were used as a basis for the classification of the particles following a similar flow chart as the one given by Lorenzo et al. [46] and EPA guidelines 2002[47]. Particles which have net intensities dominant in carbon signal were considered as carbonaceous particles. Note that carbonaceous particles were found also mixed with other elements. Pure carbon particles are assumed to be formed via a vaporization-condensation mechanism during combustion processes such as burning of diesel, coal, residual oil and biomass (Kittleson 1998[48]), while mix carbon-rich particles could have been originated in combustion processes, and mixed with particles from crustal origin, construction works and traffic emissions (brake wear, tire wear and road resuspended urban dust). The remaining particles were considered as originated from natural sources, and mostly include soil particles transported by the wind or resuspended dust. They were classified as rural particles. Aluminum silicates are the most abundant particles included in this group, which is consistent with the composition of Córdoba soils (e.g. Krohling, 1999[49]). The aluminum silicates are characterized by high contents of Si and Al and variable content of Na, K, Fe, S and/or Ca. Besides aluminum silicates, particles with high intensities in Ca, Fe, S and Si were also included in this group. *Figure 5* shows the percentage and distribution of each type of particles resulting from our classification. These results are in agreement with previous studies that point to mobile sources as the main sources of air particles pollution in Córdoba. [45]

Figure 5

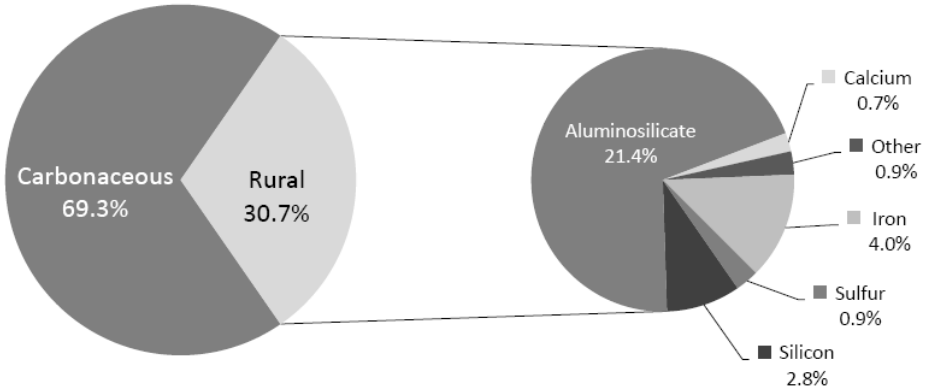

Figure 5: Distribution of the total particles analyzed by SEM in the carbonaceous and rural groups; for the rural group, the contributions from each particle type is also indicated.

TEM analysis revealed also the presence of carbonaceous particles. Large branching soot aggregates (Wu et al. 2000[50]) were obtained in urban areas. Carbonaceous particles have also been found associated with other particles. We attribute these associations to the agglomeration of mineral and combustion materials. Silica (SiO_2) aggregates were also found. These

aggregates contain spherules of black carbon bonded together in an amorphous shape and coated by organic matter (Jacobson 2005[51]). Mixed agglomerates are indicative of an aged aerosol where combustion compounds have attached to other particles in the atmosphere (Dye et al. 2000[52]). As carbonaceous particles contain mostly soot aggregates, its size and morphology were investigated using fractal theory. The ImageJ software package which is freely available (http://rsb.info.nih.gov/ij/) was used for image processing and analyzing. From the binary images the following 2D parameters of the aggregates were retrieved: fractal dimension of the projected surface area $D_{f,2D}$, projected surface area, projected maximum length L and perpendicular width W of the aggregate, the aspect ratio of the aggregate AR = L/W, the radius of primary particles r_p, and the projected surface area of primary particle Ap. These parameters were used to derive the 3D properties of the aggregates: fractal dimension D_f, the gyration prefactor k_g and the particulate diameter in nm, which are presented in *table 2*. From this table it can be seen that the measured average diameter of the primary particles in aggregates ranged between 9 and 48 nm.

Particle ID	D_f	k_g	*Particle Diameter (nm)*
1	1.91	3.38	34
2	1.81	5.16	33
3	1.95	3.6	48
4	1.86	16.42	9
5	1.87	4.28	28
6	1.86	3.2	28
7	1.89	5.29	34
8	1.95	3.66	28
9	1.64	4.65	32
10	1.7	3.81	40
11	1.95	4.34	39
12	1.76	13.65	27
13	1.46	0.89	27
14	1.87	4.83	20
15	1.93	6.49	32
16	1.91	10.65	22

Table 2

Fractal parameters of carbonaceous particles

The fractal dimensions for the soot aggregates varied from 1.46 to 1.95. Sachdeva and Attri, 2008[53] showed that the D_f for soot samples derived from different fuels varied from 1.36 to 1.88. According to these authors the aggregates derived from biomass showed low D_f value (1.27); diesel truck, 1.82; gasoline, 1.36 and diesel jeep, 1.77. The fractal dimension is important for the quantitative characterization of the aggregate morphology. Densely packed aggregates have D_f values close to 3, whereas the fractal dimension of chain-like branched clusters can be significantly smaller. The other important structural coefficient, k_g, is also related to the state of compactness of a fractal particle. For a fixed D_f, the packing density tends to be smaller as k_g decreases. It is widely believed that the fractal dimension of a soot particle reflects its history and thus is controlled by the particle source, generating conditions, and aging processes (Adachi et al. 2007[54]). Post-combustion soot exists in open chain-like structures of individual spherules (Abel et al. 2003[55]). As the aerosol ages, the chain-like aggregate tends to collapse into a more compact soot cluster (Reid and Hobbs 1998[56]). The changing morphology of soot through aging is expected to have an important effect on the predicted optical characteristics.

4. Summary

In this chapter we present the main results of the advances made in the central region of Argentina respect to the different environmental aspects of radiation, aerosols and clouds.

To accomplish that, hourly UV-B radiation values recorded between 1998 and 2011 in Córdoba city were analyzed. The agreement between UV-B irradiance measurements and TUV model calculations under clear-sky conditions was better than ±5% for SZA less than 50º and better than ±10% for SZA less than 70º. Therefore, the large reductions found in the surface radiation on cloudless days can be attributed to the effect of the aerosol loading. This effect on the UV-B irradiance was reproduced incorporating the optical properties of the aerosols provided by AERONET (AOD at 340 nm, ω_0 at 440 nm, and *g* at 440 nm) in the TUV model. The effects of different types of clouds (stratocumulus, cumulus, and cirrus) on the broadband UV-B irradiance and on the corresponding DGRs have been analyzed and differentiated by using surface broadband and spectral radiation measurements taken at the same site. A total of 16 days with stratocumulus, 12 with cumulus, and 16 with cirrus were studied using 21 clear sky days as a reference. The found averages and standard deviations for the DGRs were 1.02 ± 0.06 for stratocumulus, 0.74 ± 0.18 for cumulus, 0.63 ± 0.12 for cirrus, and 0.60 ± 0.13 for the clear sky days, respectively. TUV model was also used to evaluate the DGRs under clear sky conditions and also to assess the effects of an idealized cloud in a wide range of altitudes, SZAs, and cloud optical depths.

In parallel with the study of the effects that clouds and aerosols have on radiation; the characterization of aerosol bulk composition for Córdoba in both PM10 and PM2.5 fractions was carried out by using SR-XRF. The results of the study suggest that the coarse fraction (the difference between PM10 and PM2.5) concentration has an important contribution of ground dust or re-suspended material, which is composed mainly by aluminum silicates, while the fine fraction is enriched in toxic metals, emitted as a result of anthropogenic activities. Gravimetric analysis of the filters reveals that the main percentage of PM10 corresponds to the smallest particles, PM2.5. In addition, SEM and TEM techniques were used to characterize the elemental composition, morphology, and sizes of the individual atmospheric aerosol particles in PM2.5 and PM10 fractions. Data obtained by TEM allowed also the analysis of carbonaceous particles. Despite the differences in type of vehicles, fuels, and traffic of the different sampled sites, typical carbonaceous particles were found in all the analyzed samples. Some other particles have been found internally mixed with carbonaceous particles, especially in urban places, where the loaded filters were particularly dark. The combination of TEM and image analysis of the micrographs allowed determining the particle structure of the soot found in the aerosols of Córdoba City. The soot exhibit a fractal-like agglomerate structure and their fractal parameters were determined. Based on the results of the study and the recommendations from international air quality agencies, there is a need of an urgent government abatement policy to prevent a further exacerbation of the air pollution due to PM in the city.

5. Acknowledgments

We thank ANPCyT (Préstamo BID PICT 309), CONICET and SeCyT (UNC) for partial support of the work reported here. M.L. López and M. Achad thank CONICET and FONCyT for a Postdoctoral and Doctoral fellowships, respectively. We especially thank the PI and his staff for establishing and maintaining the AERONET Córdoba-CETT site used in this investigation. We also thank Brent Holben for permission to use the AERONET data and CONAE (Comisión Nacional de Actividades Espaciales) staff for looking after the instrument deployed in this site. We greatly appreciate the help of S. Ceppi and G. Tirao with the SR-XRF measurements and the support of the National Synchrotron Light Laboratory (LNLS), Brazil.

References

[1] McKenzie RL, Bodeker GE, Keep DJ, Kotkamp M, Evans JM. UV radiation in New Zealand: measured north to south differences, relationship to other latitudes. Weather and climate. 1996; 16: 17-26.

[2] Lubin D, Chen B, Bromwich DH, Somerville RCJ, Lee WH, Hines K. The Impact of Antarctic Cloud Radiative Properties on a GCM Climate Simulation. J. Clim. 1998; 11: 447-462.

[3] Estupiñán JG, Raman S, Crescenti GH, Streicher JJ, Barnard WF. Effects of clouds and haze on UV-B radiation. J Geophys Res. 1996; 101(D11): 16807-16816.

[4] Frederick JE, Koob AE, Alberts AD, Weatherhead EC. Empirical Studies of tropospheric transmission in the ultraviolet: broadband measurements. J. Appl. Meteorol. 1993; 32: 1883-1892.

[5] Meleti C, Cappellani F. Measurements of aerosol optical depth at Ispra: Analysis of the correlation with UV-B, UV-A, and total solar irradiance. J. Geophys. Res. 2000; 105:4971-4978.

[6] Reuder J, Schwander H. Aerosol effects on UV radiation in nonurban regions. J. Geophys. Res. 1999; 104(D4): 4065-4078.

[7] Anderson TL, Covert DS, Wheeler JD, Harris JM, Perry KD, Trost BE, Jaffe DJ, Ogren JA. Aerosol backscatter fraction and single scattering albedo: Measured values and uncertainties at a coastal station in the Pacific Northwest. J. Geophys. Res. 1999; 104: 26,793–26,807.

[8] Devaux C, Vermeulen A, Deuze JL, Dubuisson P, Herman M, Santer R. Retrieval of aerosol single-scattering albedo from ground-based measurements: Application to observational. J. Geophys. Res. 1998; 103: 8753-8761.

[9] Dubovik O, Holben BN, Kaufman YJ, Yamasoe M, Smirnov A, Tanre D, Slutsker I, Single-scattering albedo of smoke retrieved from the sky radiance and solar transmittance measured from ground. J. Geophys. Res. 1998;103:31,901–31,923.

[10] Krotkov NA, Bhartia PK, Herman J, Slusser J, Scott G, Labow G, Vasilkov A, Eck T, Dubovik O, Holben BN. Aerosol UV absorption experiment (2002-04): 2. Absorption optical thickness, refractive index, and single scattering albedo. Opt Eng. 2005; 44 (4), 041005.

[11] Kylling A., Bais AF, Blumthaler M, Schreder J, Zerefos CS, Kosmidis E. The effect of aerosols on solar UV irradiances during the photochemical activity and solar ultraviolet radiation campaign. J. Geophys. Res. 1998; 103: 26,051-26,060.

[12] Madronich S. UV radiation in the natural and perturbed atmosphere. In: Tevini M, editor. UV-B radiation and ozone depletion.Effects on humans, animals, plants, microorganisms, and materials. Boca Raton: Lewis Publisher; 1993. p. 17–69.

[13] Lacis AA, Mishchenko MI. Climate forcing, climate sensitivity, and climate response: A radiative modeling persepctive on atmospheric aerosols in: Charlson R.J. and Heintzenberg J, editors. Aerosol Forcing of Climate: Report of the Dahlem Workshop on Aerosol Forcing of Climate. Berlin: 1995. p. 24-29;

[14] Kazadzis S, Bais A, Kouremeti N, Gerasopoulos E, Garane K, Blumthaler M, Schallhart B, Cede A. Direct spectral measurements with a Brewer spectroradiometer: absolute calibration and aerosol optical depth retrieval. App Opt. 2005; 44: 1681-1690.

[15] Bais AF, Kazantzidis A, Kazadzis S, Balis DS, Zerefos CS, Meleti C. Deriving an effective aerosol single scattering albedo from spectral surface UV irradiance measurements. Atmos. Env. 2005; 39:1093–1102.

[16] Goering CD, L'Ecuyer TS, Stephens GL, Slusser JR, Scott G, Davis J, Barnard JC, Madronich S. Simultaneous retrievals of column ozone and aerosol optical properties from direct and diffuse solar irradiance measurements. J. Geophys. Res. 2005; 110: 05, D05204, 10.1029/2004JD005330.

[17] Slusser J, Krotkov N, Gao W, Herman JR, Labow G, Scott G. Comparison of USDA UV shadow-band irradiance measurements with TOS satellite and DISORT model retrievals under all sky conditions, in: Slusser J.R. et al. (eds.), Ultraviolet Ground- and Space-based Measurements, Models an Effects, SPIE Proc. 2001; 56–69.

[18] Dockery DW, Pope 3rd. CA. Acute respiratory effects of particulate air pollution. Annual Review of Public Health. 1994;15: 107-132.
[19] Smichowski P, Gómez D, Dawidowski L. Giné M, Sánchez Bellato S, Reich S, Monitoring trace metals in urban aerosols from Buenos Aires City. Determination by plasma-based techniques. J. Env. Monit. 2004; 6: 286-294.
[20] Suzuki K. Characterization of airborne particulates and associated trace metals deposited on tree bark by ICP-OES, ICP-MS, SEM-EDX and laser ablation ICP-MS. Atmos. Env. 2006; 40: 2226-2234.
[21] Olcese LE, Toselli BM. Unexpected high levels of ozone measured in Córdoba, Argentina. J. Atm. Chem. 1998; 31: 269–279.
[22] Palancar GG, Toselli BM. Erythemal ultraviolet irradiance in Córdoba, Argentina. Atmos. Env. 2002; 36: 287–292
[23] Holben BN, Tanré D, Smirnov A, Eck TF, Slutsker I, Abuhassan N, Newcomb WW, Schafer J, Chatenet B, Lavenue F, Kaufman YJ, Vande Castle J, Setzer A, Markham B, Clark D, Frouin R, Halthore R, Karnieli A, O'Neill NT, Pietras C, Pinker RT, Voss K, Zibordi G. An emerging ground-based aerosol climatology: Aerosol Optical Depth from AERONET. J. Geophys. Res. 2001; 106:12 067-12 097.
[24] Dubovik O, Smirnov A, Holben BN, King MD, Kaufman YJ, Eck TF, Slutsker I, 2000. Accuracy assessments of aerosol optical properties retrieved from AERONET sun and sky-radiance measurements. J. Geophys. Res. 2000; 105: 9791-9806.
[25] Draxler RR, Hess, GD, An overview of the HYSPLIT-4 modelling system for trajectories, dispersion and deposition. Austral. Meteorol. Mag. 1998; 47: 295-308.
[26] Draxler, RR. Evaluation of an ensemble dispersion calculation, J. Appl. Meteorol. 2003; 42: 308-317.
[27] Vana M, Tamm E. Propagation of atmospheric aerosol and the area of representativeness of its measurements in the Baltic Sea region. Atmos. Env. 2002; 36: 391–401.
[28] Gassmann M, Pérez CL.. Trajectories associated to regional and extra-regional pollen transport in the southeast of Buenos Aires province, Mar del Plata. Argentina, Int. J. Biometeorol. 2006; 50, 280–291.
[29] McGowan H, Clark A. Identification of dust transport pathways from Lake Eyre, Australia using Hysplit. Atmos. Env. 2008; 42: 6915–6925.
[30] Madronich S. Photodissociation in the atmosphere 1. Actinic flux and the effects of ground reflections and clouds. J. Geophys. Res. 1987; 92(D8): 9740-9752.
[31] Madronich S, Flocke S. Theoretical estimation of biologically effective UV radiation at the Earth's surface, in: Zerefos CS et al. editors. Solar Ultraviolet Radiation - Modeling, Measurements and Effects, NATO ASI Series, Springer-Verlag, Berlin; 1997. p. 23-48.
[32] Palancar GG, 2003. Estudio de procesos cinéticos y radiativos de interés atmosférico. Ph. D. Thesis, Universidad Nacional de Córdoba, Argentina.
[33] Van Hoosier ME, Bartoe JD, Brueckner GE, Printz DK. Solar Irradiance measurements 120–400 nm from Space Lab-2. IUGG Assembly, Vancouver.1987.
[34]Neckel H, Labs D. The solar radiation between 3300 and 12500 Å. Solar Phys. 1984; 90:205-258.
[35] Olcese LE, Toselli BM. Some aspects of air pollution in Córdoba, Argentina. Atmos. Env. 2002; 36: 299-306.
[36] Elterman L, UV, visible, and IR attenuation for altitudes to 50 km. Environmental Research Papers. Report 68-0153, Air Force Cambridge Research Laboratories. 1968. p.285.
[37] López ML, Palancar GG, Toselli, BM, Effect of different types of clouds on surface UV-B and total solar irradiance at southern mid-latitudes: CMF determinations at Córdoba, Argentina. Atmos. Env. 2009; 43: 3130-3136.
[38] López ML, Palancar GG, Toselli, BM, Effects of stratocumulus, cumulus, and cirrus clouds on the UV-B Diffuse to Global Ratio: experimental and modeling results. J. Quant. Spectrosc. Radiat. Transfer. 2012; 113: 461-469.

[39] Zuidema P, Painemal D, De Szoeke S, Fairall C. Stratocumulus cloud top height estimates and their climatic implications. J. Clim. 2009; 22: 4652-4666.
[40] Palancar GG, Toselli BM. Effects of meteorology and tropospheric aerosols on UV-B radiation: a 4-year study. Atmos Env. 2004; 38: 2749-2757.
[41] Andrada GC, Palancar GG, Toselli BM. Using the optical properties of aerosols from the AERONET database to calculate surface solar UV-B irradiance in Córdoba, Argentina: Comparison with measurements. Atmos. Env. 2008; 42: 6011-6019.
[42] Olcese LE, Toselli BM. Effects of meteorology and land use on ambient measurements of primary pollutants in Córdoba City, Argentina. Meteorol. Atmos. Phys. 1997; 62: 241-248.
[43] Palancar GG, Toselli BM. Effects of meteorology on the annual and interannual cycle of the UV-B and total radiation in Córdoba city, Argentina. Atmos. Env. 2004; 38: 1073-1082.
[44] Air Quality Criteria for Particulate Matter. U.S. EPA/600/P-99/002aF-bF. 2004; 1.1-1.20.
[45] López ML, Ceppi S, Palancar GG, Olcese LE, Tirao G, Toselli B M. Elemental concentration and source identification of PM10 and PM2.5 by SR-XRF in Córdoba, Argentina. Atmos. Env. 2011; 45: 5450-5457.
[46] Lorenzo R, Kaegia R, Gehriga R, Grobety B. Particle emissions of a railway line determined by detailed single particle analysis. Atmos. Env. 2006; 40: 7831-784.
[47] Willis RD, Blanchard FT, Conner TL. Guidelines for the Application of SEM/EDX Analytical Techniques to Particulate Matter Samples. U.S. EPA/ 600/R-02/070. 2002.
[48] Kittleson DB. Engines and nanoparticles: a review. J. Aerosol Sci. 1998; 29:575-588.
[49] Krohling DM. Sedimentological maps of the typical loessic units in North Pampa, Argentina. Quaternary Int. 1999; 62: 49-55.
[50] Wu Q, Xue Z, Qi Z, Wang F. The microscopic morphology of highly sulfonated polyaniline. Synthetic Metals. 2000; 108:107-110.
[51] Jacobson MZ. Fundamentals of Atmospheric Modeling. United Kingdom : University Press; 2005.
[52] Dye AL, Rhead MM, Trier CJ. The quantitative morphology of roadside and background urban aerosol in Plymouth, UK. Atmos. Env. 2000; 34: 3139-3148.
[53] Sachdeva K, Attri AK. Morphological characterization of carbonaceous aggregates in soot and free fall aerosol samples. Atmos. Env. 2008; 42:1025-1034.
[54] Adachi K, Chung SH, Friedrich H, Buseck PR. Fractal parameters of individual soot particles determined using electron tomography: implications for optical properties. J. Geophys. Res. 2007; 112: D14202.
[55] Abel SJ, Haywood JM, Highwood EJ, Li J, Buseck PR. Evolution of biomass burning aerosol properties from an agricultural fire in southern Africa. Geophys. Res. Lett.2003; 30: 1783.
[56] Reid JS, Ob. PV. Physical and optical properties of young smoke from individual biomass fires in Brazil. J. Geophys. Res. 1998; 103: 32013-30.